A Novel Dual-Band SIW Filter with High Selectivity

Yu-Dan Wu, Guo-Hui Li[*], Wei Yang, and Tong Mou

Abstract—A novel dual-band substrate integrated waveguide (SIW) filter with multiple transmission zeros and good out-of-band rejection performance is presented in this paper. For this purpose, an orthogonal input/output (I/O) feeding structure directly connected to the substrate integrated waveguide (SIW) cavity is designed to split the resonant frequencies of the degenerate pair of mode. The filter can be modeled with a multi-path circuit formed by three modes (TE_{101}, TE_{201} and TE_{102} modes) and weak cross coupling between I/O ports, thereby producing three transmission zeros which make the dual-band high selectivity. The offset of the input/output ports shifts the second transmission zero to a lower frequency from the upper passband. Several filter prototypes are designed and fabricated for demonstration, and the measured results validate the new structure for high selectivity applications.

1. INTRODUCTION

Microwave filters are key components in modern communication systems. Recent advances in communication technologies bring about the requirement of highly selective microwave filters with compact size, low cost, high power capability, etc. Transmission lines, such as microstrip, coplanar waveguide (CPW) and rectangular waveguide, have been used in the design of microwave filters. Compared with these structures, substrate integrated waveguide (SIW) has attracted much attention for its low cost, high performance and flexible integration with radio-frequency/microwave integrated circuits. Recently, half-mode SIW, folded half-mode SIW and quarter-mode SIW have been widely employed for designing filter with size reduction [1–4]. For a bandpass response technology, slots loaded on SIW cavity attract lot of academic attention for its easy design and fabrication [5, 6].

Dual-band bandpass filter is an indispensable component for multi-band systems since it can be used as two separate single bandpass filters. So far, several ways have been used to acquire dual-band. Traditionally, a dual-band filter is based on degenerate modes of a cavity or the frequency transformation from normalized frequency domain [7]. In [8], dual-band is realized by generating one transmission zero in the middle of a wide passband. Li et al. proposed a dual-band SIW filter based on spirality compact microstrip resonators cell [9]. A three-cavity dual-mode dual-band filter is designed using coupling matrix [10]. Dual-band filters using metamaterials [11], defected ground structure (DGS) [12] and complementary split ring resonator (CSRR) [13, 14] are introduced.

In this paper, a novel dual-band (SIW) filter is presented, and the dual-band response is realized by open loop resonators, TE_{101} mode and the first degenerate modes (TE_{201} and TE_{102}). By using an orthogonal input/output feeding line for perturbation, the generated TE_{102} and TE_{201} modes are split. Two open loop resonators etched on the substrate integrated waveguide (SIW) cavity not only are used as resonators but also generate inter-coupling. The proposed bandpass filter is analyzed and designed using full-wave EM simulator software (Ansoft HFSS). To validate the design and analysis, several filter prototypes are designed and fabricated. The measured results verify the performance of the proposed filters.

2. FILTER DESIGN

2.1. Basic Structure of SIW Resonant Cavity (Filter I)

Figure 1 shows the configuration of filter I. It is composed of an SIW square resonant cavity etching with two open loop resonators (OLRs). It is also used as a basic structure in this paper. According to the formula given by [12], the size of the cavity is adjusted to a suitable cut off frequency f_c, where a and h are the length and height of the cavity, respectively, d is the diameter of the metallic vias, $l1 \sim l2$ along with $w1 \sim w2$ represent the length and width of each side of open loop resonators, $l5$ is the distance between the open loop resonator and the first vias, and $l3$ is the length between the open loop resonator and the I/O ports. The width of I/O ports is wp and the width of open loop resonators is $s0$. The main parameters to be optimized in this structure are given as: $a = 25.45$ mm, $d = 1$ mm, $h = 0.508$ mm, $l1 = 5.25$ mm, $l2 = 3$ mm, $l3 = 1$ mm, $l5 = 5.2$ mm, $w1 = 0.8$ mm, $w2 = 1.86$ mm, $wp = 1.52$ mm, $s0 = 0.2$ mm.

The open loop resonators etched on SIW cavity not only are used as resonators but also generate inter-coupling. Both OLRs can take the approximated values of half-wavelength at the center frequency. The SIW and OLRs interact with each other at $l5$, thus $l5$ should be one of the adjusting parameters to be specified in Section 2.3. The embedding OLRs are placed along with the axial direction. It is worth mentioning that the width of OLRs should not be too large or the current distribution will be interfered.

The $50\,\Omega$ microstrip lines are directly connected to the SIW cavity at the input and output ports. The dual-mode resonator in Fig. 1 is formed by a pair of orthogonal input/output feeding lines for perturbation. Two degenerate resonant modes may be split by introducing a perturbation element in a resonator, and thus three modes (TE_{101}, TE_{102} and TE_{201} mode) exist in the SIW cavity. One transmission zero is created because of the opposite phase of TE_{102} and TE_{201} mode. Two additional transmission zeros are attributed to the existence of a weak cross coupling path between the input/output ports. Thus three transmission zeros will appear.
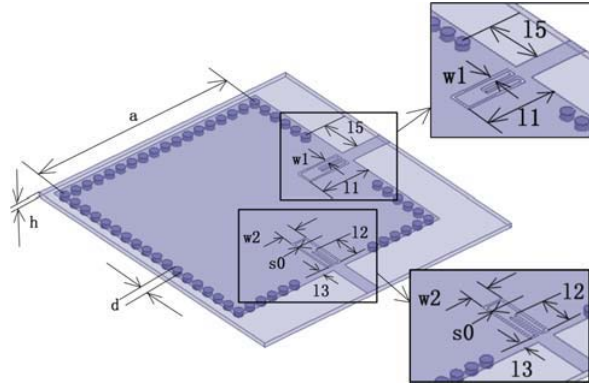
Figure 1. Structure of the square SIW cavity.

According to the above discussion, a single band and two dual-band bandpass filters are designed, fabricated and measured. This whole work is based on full wave software Ansoft HFSS. A 0.508 mm thick Rogers 5880 is used in this paper with a relative permittivity of 2.2, dielectric loss tangent of 0.0009. The diameter of the vias is 1 mm and the space between two vias is 1.5 mm (only for filter I).

The simulated and measured frequency responses for filter I are shown in Fig. 2. As described above, the center frequency is located at 5.4 GHz and the bandwidth is about 6.5%. It can be seen that the second spurious response appears at 8.5 GHz, about only 1.57 times of the first resonant frequency. Three transmission zeros can be observed to improve the selectivity. It should be noted that this filter suffers from poor performance. It is used as a basic structure for the next two dual-band bandpass filters to be specified in Section 2.2 and Section 2.3.

(a)   (b)
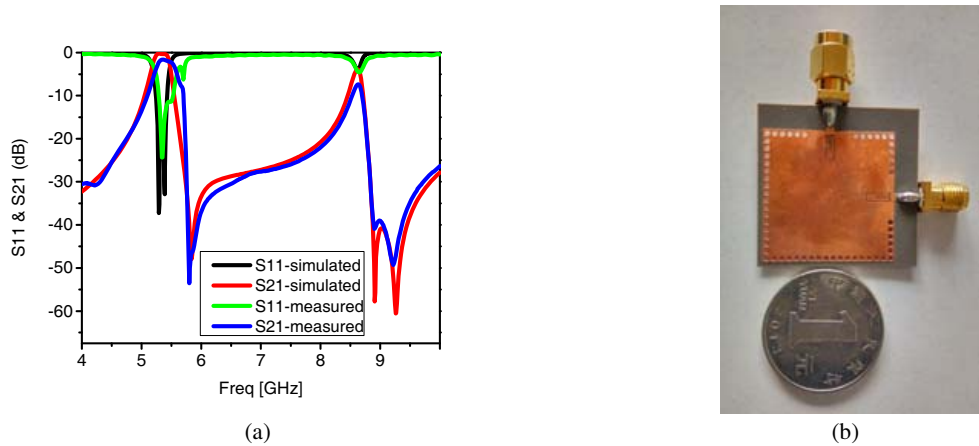
Figure 2. The single band bandpass filter I. (a) Simulated and measured frequency responses. (b) Top-view photograph.

2.2. Design of Dual-Band Bandpass Filter II

To demonstrate the application of the proposed SIW resonator, a dual-band bandpass filter with a circular slot is investigated. Fig. 3 shows the configuration of filter II. The circular slot is just located at the center of the SIW cavity. The inner and outer radius of the slot are $r1$, $r2$, respectively.
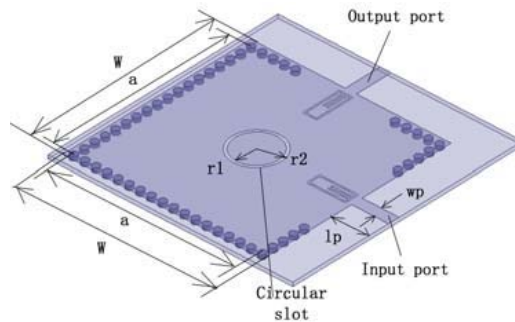
Figure 3. Configuration of the proposed dual-band bandpass filter II.

The circular slot etched on SIW cavity is about a half-wavelength to control the frequency response of the resonator. As is know to all, the coupling between the two degenerate modes can be used to build a bandpass filter. The circular slot is employed here to enhance the coupling between TE_{201} and TE_{102} modes, while the coupling can be adjusted by different value of radius. Thus the second passband of filter II is formed. But the radius of the circular slot should not be too big to avoid interference with the first degenerate mode.

The dimensions in Fig. 3 are chosen as follows (all in mm): $a = 25.45$, $d = 1$, $h = 0.508$, $l1 = 5.25$, $l2 = 3$, $l3 = 0.85$, $l5 = 5.2$, $w1 = 0.8$, $w2 = 1.86$, $wp = 1.52$, $W = 27.05$, $r1 = 2.95$, $r2 = 3.3$, $s0 = 0.2$. The overall size of the device, including the input/output feeding lines is about $30\,\text{mm} \times 30\,\text{mm}$. As shown in Fig. 4(a), the lower passband and upper passband are centered at 5.2 GHz and 7.8 GHz, respectively. The photograph of the fabricated dual-band filter is shown in Fig. 4(b).

2.3. Design of Dual-Band Bandpass Filter III

Filter III is another design based on the basic SIW resonant cavity mentioned in Section 2.1. Configuration of the filter is shown in Fig. 5. The only difference with the basic structure (Fig. 1) is that the centers of the two open loop resonators are not located right on the X-axis and Y-axis,

(a)   (b)
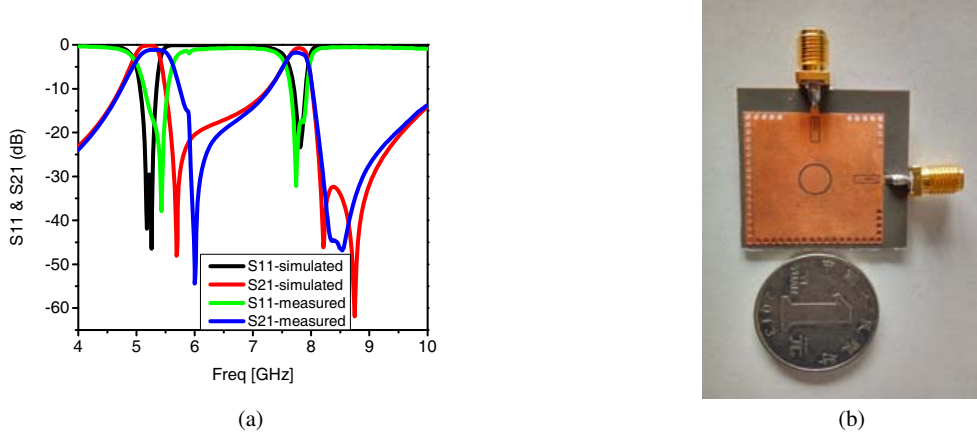
Figure 4. The dual-band bandpass filter II. (a) Simulated and measured frequency responses. (b) Top-view photograph.
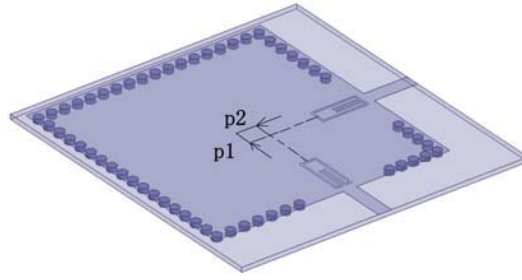
Figure 5. Configuration of the proposed dual-band bandpass filter III.

(a)   (b)
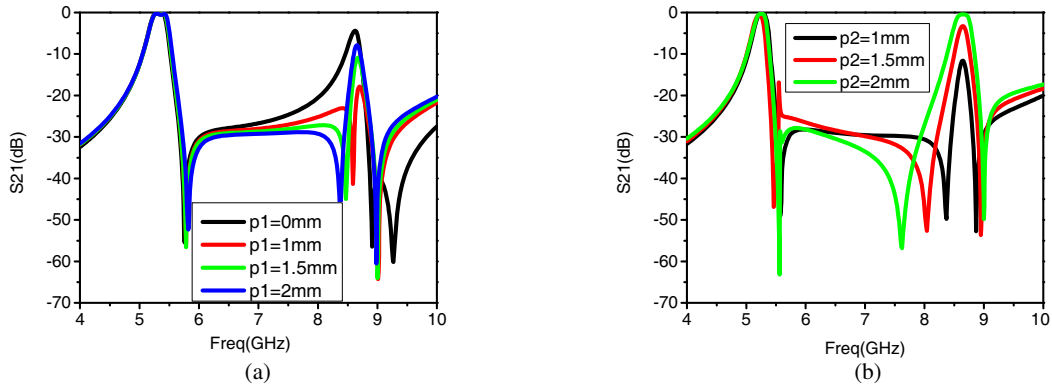
Figure 6. Frequency responses of filter III with various $p2$ and $p1$ values. (a) versus $p1$ ($p2 = 0\,\text{mm}$) (b) versus $p2$ ($p1 = 2\,\text{mm}$).

where they are shifted with a deviation of $p1$ and $p2$. According to [15], the position of I/O ports in a cavity is the main design parameter to control the transmission zeros and its position with respect to the passband. Fig. 6 demonstrates the bandwidth control according to the change in deviation of $p1$ and $p2$. As shown in Fig. 6 (a), as $p1$ increases, the first transmission zero remains almost the same while the location of the second transmission zero moves to lower frequency from upper passband. The location of second passband is decided by the deviation of $p1$. Thus, the performance of out-of-band rejection of the second passband will be greatly improved with an appropriate deviation of $p1$, whereas the first passband remain stationary. According to Fig. 6 (b), $p2$ controls the S-parameter S_{21} of the second

passband. Meanwhile, it also has an extremely effect on the location of the second transmission zero when $p1$ is fixed. After making a compromise of return loss and the location of the second transmission zero, when $p1$ and $p2$ are fixed at 2 mm, three transmission zeros appear at 5.7 GHz, 7.6 GHz and 9 GHz, resulting in high selectivity.

The SIW and open loop resonators interact with each other which have been mentioned in Section 2.1. As demonstrated in Fig. 7, $l5$ controls the location of the first transmission zero with nearly no influence upon the second passband.
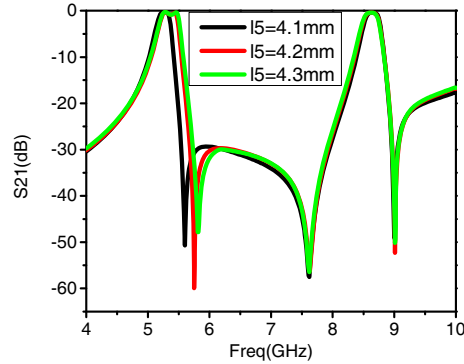
Figure 7. Frequency responses of filter III under different values of $l5$.

Table 1. Comparison between filter III and the references.

	Order	f_0 (GHz)	IL (dB)	FBW (%)
[5]	8	5.9/6.1	2/2.4	1.8/1.7
[7]	3	3.58/5.875	1.57/1.75	6.97/1.19
[8]	3	5.85/6.15	2.2/2	1.3/1.3
This work	5	5.3/8.7	1.8/1.94	6.8/ 3.2

The corresponding structure parameters in Fig. 5 are given as: $a = 25.45$ mm, $d = 1$ mm, $h = 0.508$ mm, $l1 = 5.25$ mm, $l2 = 3.2$ mm, $l3 = 1$ mm, $l5 = 4.2$ mm, $w1 = 0.79$ mm, $w2 = 1.86$ mm, $wp = 1.52$ mm, $W = 27.05$ mm, $p1 = 2$ mm, $p2 = 2$ mm, $s0 = 0.2$ mm. The size of the device is the same as that of filter II. In Fig. 8, both the measured and simulated results are presented.

A comparison of the dual-band SIW filters ([7, 9, 10]) to the proposed filter III is shown in Table 1. It can be seen that filter III has a good performance of small return loss, wide band, good return loss, high selectivity and easy design and fabrication, though its upper stopband is not very outstanding (20 dB @ 9.75 GHz).

3. FABRICATION AND EXPERIMENT

The proposed bandpass filters are analyzed and designed using full-wave EM simulator software (Ansoft HFSS). To validate the design and analysis, the filter prototypes were designed and fabricated. The fabricated filters were measured using Agilent 8722ES network analyzer. The measured results were plotted together with those simulated ones. Good agreements between the simulated and measured results have been obtained. The measured results are listed in Table 2. It should be pointed out that although the agreement of the measured response with the simulated frequency responses is acceptable, discrepancies can be observed from the Table: The measured in-band return losses are 5∼10 dB (for three filters) smaller than the simulation ones. It also can be observed that the center frequencies have a relative offset to higher frequency and the bandwidths of the first passband are larger than that of the simulation while the second passbands are nearly the same. Here, we further discuss the changing properties of the proposed filter at different values of $s0$. Considering the simulated frequency responses

of the filters with different values of $s0$, as shown in Fig. 9 (filter II is taken as an example), the first center frequency drift is observed. Hence, the offset of the center frequency is caused by the precision of $s0$ in the fabrication process (within the tolerance of the etching machine). It is conjectured that the unsatisfactory return loss may be attributed to slight impedance mismatch between the feeding section and the SMA connectors caused by manual welding and the effective conductivity of fabricated filters which is less than that of the simulation.

It should be noted that filter III has the most excellent performance for its high selectivity which is realized by three transmission zeros located at 5.7 GHz with a 51 dB rejection, 7.6 GHz with a 42 dB rejection, and 9.0 GHz with a 45 dB rejection, respectively. The measured results show that the lower passband and upper passband are centered at 5.3 and 8.7 GHz, with insertion losses of < 1.8 dB and < 1.94 dB. The rejection is more than 31.9 dB in the stopband which lies between the dual passband from 5.77 GHz to 7.64 GHz. In addition, the filter III has the fractional bandwidth of about 6.8%/3.2% at 5.3 GHz/8.7 GHz.

Table 2. The measured results of the proposed filters.

	$f0$ (GHz)	IL (dB)	FBW (%)	RL (dB)
Filter I	5.4	1.61	6.5	11.6
Filter II	5.3/7.75	1.16/1.76	11.8/5.4	19.2/17.2
Filter III	5.3 /8.7	1.8/1.94	6.8/3.2	17.6/22.3
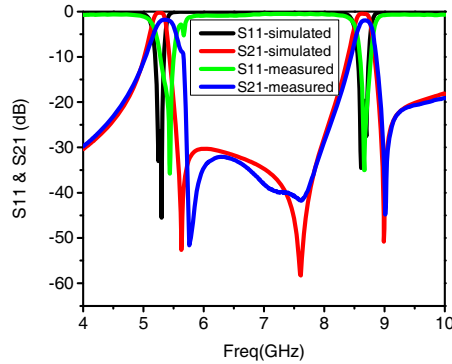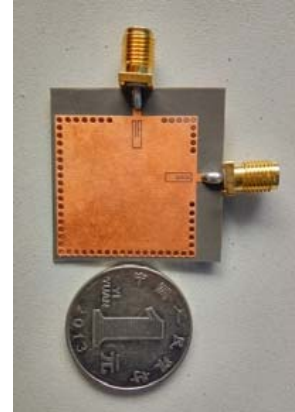
(a)   (b)

Figure 8. The dual-band bandpass filter III. (a) Simulated and measured frequency responses. (b) Top-view photograph.
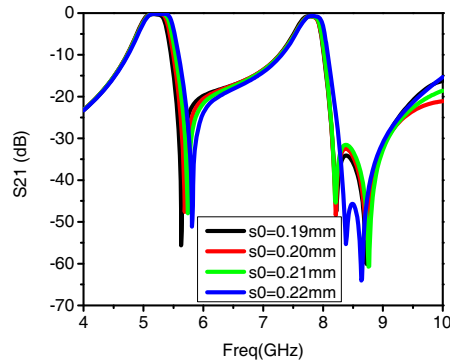
Figure 9. Frequency responses of under different values of $s0$.

4. CONCLUSION

A novel open loop resonator allows the design of extremely compact high selectivity SIW bandpass filter. Three filters were proposed and fabricated, which show different bandpass responses. Filter I possesses the property of single band bandpass with high mode spurious. Low insertion loss and wideband can be realized for dual-band filter II with a circular slot etched on the basic SIW structure, but the out-of-band performance of the second passband is not outstanding. Compared with previous two filters, filter III exhibits an excellent out-of-band rejection performance. The first and second transmission zeros can be independently controlled to desired values by tuning the dimensions of open loop resonators. All of the filters are fabricated on a 0.508 mm-thickness F4B substrate based on the proposed SIW cavity. Both simulated and measured results suggest that the proposed SIW cavity is a candidate for the design of compact planar dual-band filters.

ACKNOWLEDGMENT

REFERENCES

1. Chien, H. Y., T. M. Shen, T. Y. Huang, et al., "Miniaturized bandpass filters with double-folded substrate integrated waveguide resonators in LTCC," *IEEE Transactions on Microwave Theory & Techniques*, Vol. 57, No. 7, 1774–1782, 2009.

2. Sekar, V. and K. Entesari, "A novel compact dual-band half-mode substrate integrated waveguide bandpass filter," *IEEE MTT-S International Microwave Symposium Digest. IEEE MTT-S International Microwave Symposium*, 1–4, 2011.

3. Sekar, V. and K. Entesari, "Miniaturized half-mode substrate integrated waveguide bandpass filters using cross-shaped fractals," *2011 IEEE 12th Annual. IEEE Wireless and Microwave Technology Conference (WAMICON)*, 1–5, 2011.

4. Zhang, X., C. Ma, and F. Wang, "Design of compact dual-passband LTCC filter exploiting stacked QMSIW and EMSIW," *Electronics Letters*, Vol. 51, No. 12, 912–914, 2015.

5. Chu, P., L. Hong, L. Dai, et al., "A planar bandpass filter implemented with a hybrid structure of substrate integrated waveguide and coplanar waveguide," *IEEE Transactions on Microwave Theory & Techniques*, Vol. 62, No. 2, 266–274, 2014.

6. Chen, R. S., S. W. Wong, L. Zhu, et al., "Wideband bandpass filter using u-slotted substrate integrated waveguide (SIW) cavities," *IEEE Microwave & Wireless Components Letters*, Vol. 25, No. 1, 1–3, 2015.

7. Chen, J., B. Wu, L. W. Jiang, et al., "Design of dual-band substrate integrated waveguide filter using frequency transformation method," *2010 International Conference on Microwave and Millimeter Wave Technology (ICMMT)*, 1286–1289, 2010.

8. Lenoir, P., S. Bila, F. Seyfert, et al., "Synthesis and design of asymmetrical dual-band bandpass filters based on equivalent network simplification," *IEEE Transactions on Microwave Theory & Techniques*, Vol. 54, No. 7, 3090–3097, 2006.

9. Li, D., C. M. Tong, P. Peng, et al., "A novel miniaturized and dual-band filter of substrate integrated waveguide based on SCMRC," *2013 Cross Strait Quad-Regional Radio Science and Wireless Technology Conference (CSQRWC)*, 82–85, 2013.

10. Rezaee, M. and A. R. Attari, "A novel dual mode dual band SIW filter," *2014 44th European IEEE Microwave Conference (EuMC)*, 853–856, 2014.

11. Turgaliev, V., D. Kholodnyak, I. Vendik, et al., "A novel dual-bandpass microwave filter using espilon-near-zero metamaterials," *2013 7th International Congress on IEEE Advanced Electromagnetic Materials in Microwaves and Optics (Metamaterials)*, 136–138, 2013.

12. Wang, Z. D., F. Wei, L. Zhang, et al., "Design of dual-band bandpass SIW filter with DGS," *2012 International Conference on Microwave and Millimeter Wave Technology (ICMMT)*, 1–3, 2012.

13. Senior, D. E., X. Cheng, M. Machado, et al., "Single and dual band bandpass filters using complementary split ring resonator loaded half mode substrate integrated waveguide," *2010 IEEE Antennas and Propagation Society International Symposium (APSURSI)*, 1–4, 2010.

14. Dong, Y. and T. Itoh, "Miniaturized dual-band substrate integrated waveguide filters using complementary split-ring resonators," *2011 IEEE MTT-S International IEEE Microwave Symposium Digest (MTT)*, 1–4, 2011.

15. Salehi, M., J. Bornemann, and E. Mehrshahi, "Compact folded substrate integrated waveguide filter with non-resonating nodes for high-selectivity bandpass applications," *2013 European IEEE Microwave Conference (EuMC)*, 155–158, 2013.